Am J Transl Res 2021;13(10):11126-11143
www.ajtr.org /ISSN:1943-8141/AJTR0132792

Original Article

Screening of differentially expressed miRNAs during osteogenic/odontogenic differentiation of human dental pulp stem cells exposed to mechanical stress

Yani He[1,2*], Xiaoyue Guan[1,2*], Yang Du[3], Guanzhi Liu[4], Yingxue Li[1,2], Zhichen Wei[1,2], Chen Shi[1,2], Jianmin Yang[1], Tiezhou Hou[1,2]

[1]The Key Laboratory of Shaanxi Province for Craniofacial Precision Medicine Research, College of Stomatology, Xi'an Jiaotong University, Xi'an 710004, Shaanxi, P. R. China; [2]Department of Endodontics, Stomatological Hospital, College of Medicine, Xi'an Jiaotong University, Xi'an 710004, Shaanxi, P. R. China; [3]Department of Stomatology, Taihe Hospital, Shiyan 442008, Hubei, P. R. China; [4]Bone and Joint Surgery Center, The Second Affiliated Hospital of Xi'an Jiaotong University, Xi'an 710004, Shaanxi, China. [*]Equal contributors.

Received March 4, 2021; Accepted July 30, 2021; Epub October 15, 2021; Published October 30, 2021

Abstract: MicroRNAs (miRNAs) have been demonstrated as crucial transcriptional regulators in proliferation, differentiation, and tumorigenesis. The comprehensive miRNA profiles of osteogenic/odontogenic differentiation of human dental pulp stem cells (hDPSCs) under the condition of mechanical stress remains largely unknown. In this study, we aimed to discover the miRNA expression profiles of hDPSCs exposed to mechanical stress under the osteogenic/odontogenic process. We found that mechanical stress (0.09 MPa and 0.18 MPa, respectively, 30 min/day) significantly promoted the proliferation of hDPSCs since the fifth day. The expressions of DSPP, DMP1, and RUNX2 were significantly increased on day 7 in the presence of 0.09 MPa and 0.18 MPa mechanical stress. On day 14, the expression levels of DSPP, DMP1, and RUNX2 were decreased in the presence of mechanical stress. Among 2578 expressed miRNAs, 5 miRNAs were upregulated and 3 miRNAs were downregulated. Six hub target genes were merged in protein-protein interactions (PPI) network analysis, in which existed only one sub-network. Bioinformatics analysis identified an array of affected signaling pathways involved in the development of epithelial and endothelial cells, cell-cell junction assembly, Rap1 signaling pathway, regulation of actin cytoskeleton, and MAPK signaling pathway. Our results revealed the miRNA expression profiles of osteogenic/odontogenic differentiation of hDPSCs under mechanical stress and identified eight miRNAs that were differentially expressed in response to the mechanical stress. Bioinformatics analysis also showed that various signaling pathways were affected by mechanical stress.

Keywords: miRNAs, mechanical stress, odontogenic, osteogenic differentiation, DPSCs

Introduction

Irreversible pulpitis is a very common oral disease worldwide and mainly caused by bacterial infection. Currently, the major clinical treatment is the root canal therapy (RCT), intending to remove the infected pulp tissues and protect the decontaminated tooth from future bacterial infection. The pulp tissues are crucial and play vital roles in terms of nutrition, regeneration, and support of teeth since they are consisting of nerves, blood vessels, and some other cells. Thus, RCT will lead to increased brittleness of the remaining tooth tissue, reduced biologic properties of the tooth, and increased risk of tooth fracture or splitting, eventually resulting in tooth loss. With the features of stem cells, accumulated studies have demonstrated that the human dental pulp stem cells (hDPSCs) can be differentiated into osteogenic and odontogenic cells. To shed light on the clinical implications of hDPSCs in the RCT, for instance, the regeneration of teeth and pulp from these cells [1-5]. Studies have revealed that hDPSCs play critical roles in dental pulp self-defensive and restoration responses under external challenges, such as trauma, caries, and abrasion [5-9].

Given the osteogenic/odontogenic potential of hDPSCs, recent studies have investigated the

effects of external factors, such as growth factors, biological scaffold material, and mechanical stimulation, on the differentiation of hDPSCs, and demonstrated the ability of these factors in modulating the osteogenic/odontogenic differentiation of hDPSCs [10]. Considering the side effects resulted from some of these external factors, namely the inflammation and necrosis in pulp tissue caused by the traditional pulp capping drug and calcium hydroxide. It turns out that the mechanical stimulation may bring much weaker side effects as compared to the other factors, indicating it may be a better way to stimulate the osteogenic/odontogenic differentiation of hDPSCs in the aspect of pulp tissue engineering [11-14]. Recently, several studies have reported the effects of different mechanic stimulations, including fluid shear force, positive pressure, hydrostatic pressure, centrifugal force, and unidirectional longitudinal or horizontal tensile force, on the differentiation of DPSCs [15]. For example, by applying the hydrostatic pressure (HSP) (0.5 Hz and 2.5 MPa for 2 h/day) on hDPSCs for two weeks, Yu et al. found that HSP promoted odontogenic differentiation by increasing mineralization, hard tissue regeneration *in vivo*, and BMP-2 responsiveness [16]. Using the human dental pulp cells, Lee et al. showed that mechanical stress promoted odontoblastic differentiation of these cells by regulating the NF-E2-related transcription factor 2 (Nrf2)-mediated heme oxygenase-1 (HO-1) pathway [11]. When giving the centrifugal force to human stem cells from apical papilla at 200 g, 250 g, and 300 g for 30 min/d, after 7 days, the odontogenic differentiation of the cells was observed [17]. In contrast, the mechanical stretch has opposite effects on hDPSCs in terms of odontogenic differentiation. The expose of cultured DPSCs to uniaxial stretch leads to the inhibition of osteogenic differentiation but the promotion of rat DPSCs proliferation, suggested that the mechanical stretch may be a useful tool for amplifying the number of DPSCs *in vitro* for regeneration medicine [18]. To study the effects of the pulp cavity pressure on DPSCs *in vitro*, the mechanical loading models are widely used in the field to address the questions.

It has been shown that mechanical stresses can promote the odontogenic differentiation of DPSCs. The underlying mechanisms remain unclear, particularly the regulated function of non-coding RNAs (ncRNAs), for instance, miRNAs. MiRNAs mainly act as post-transcriptional regulators that inhibit the expression of their target genes and mediate many biologic processes including bone homeostasis (the balance between osteoblastogenesis and osteoclastogenesis) in normal and inflammatory microenvironments *in vivo* [19, 20]. Few studies have investigated the roles of mechanical stresses in mediating the expression of miRNAs associated with bone homeostasis. The cyclic mechanical stretch has been shown to induce osteoblastic differentiation by down-regulating the expression of miR-103a, which functions as an endogenous attenuator of RUNX2 in osteoblasts, leading to osteoblast differentiation [21]. When the stretch force to periodontal ligament stem cells is applied, this stretch force led to osteoblastic differentiation and altered the expression levels of several miRNAs, including miR-1246, a newly identified target of p53 [22]. Several other miRNAs have also been associated with osteogenic differentiation regulated by mechanical forces, such as miR-195-5p and miR-154-5p [23, 24]. Taking all these together, miRNAs play crucial roles in osteoblastic differentiation, and partly explain how mechanical forces promote bone formation.

To investigate the effects of mechanical loading on hDPSCs during the clinical operation, the various mechanical loading models have been employed *in vitro* to address the questions based on the research purposes [15]. MicroRNAs (miRNAs) are important translational regulators. Previous studies have provided evidence that miRNAs, such as miR-21 and miR-143-5p, were involved in odontoblast and/or osteoblast differentiation of hDPSCs [25, 26]. The miRNA profiles during the process of osteogenic/odontogenic differentiation of hDPSCs under the condition of mechanical stress are poorly defined. In the present study, we performed miRNA array analysis on the samples of the osteogenic/odontogenic differentiation of hDPSCs exposed to mechanical stress. We observed that, out of 2578 expressed miRNAs, eight miRNAs were differentially expressed in response to mechanical stress. The related functional network and the affected signal pathways were analyzed as well.

Materials and methods

Isolation, culture, and identification of hDPSCs

Isolation of human dental pulp tissues: The experiment was approved by the Biomedical Ethics Committee, School of Medicine, Xi'an Jiaotong University (XJTU) (No. 2020-1385). All the donors or guardians volunteered to donate their dental pulp tissues and had their teeth removed for the study with written informed consent. All healthy dental pulp tissues used for hDPSCs isolation were obtained from premolars or third molars extracted for orthodontic reasons (12 to 24 years of age) in the Stomatological Hospital, College of Medicine, XJTU, China. All participants were free of any clinical symptoms of recent infection or diseases.

Cell culture and subculture: The teeth were washed in sterile PBS. Then dental pulp tissues were collected from donated teeth, broken by a hammer, and cut into 1-2 mm^3 small pieces. The tissues were digested with 3 mg/ml type I collagenase (Gibco, USA) and 4 mg/ml dispase II (Roche, Switzerland) for 30 minutes at 37°C [27, 28]. After the termination of digestion, tissues and cells were resuspended in growth medium at 37°C in a humidified atmosphere of 5% CO_2 and 95% air until lots of cells grew out from tissue patches and approached confluence. The growth medium, which consisted of α-MEM (Hyclone, USA), 10% fetal bovine serum (FBS; Gibco, USA), 0.3 μg/ml glutamine (Gibco, USA), and 1% antibiotic-antimycotic (Gibco, USA), was changed every three days. When the cells reached 70-80% confluence, they were digested with 0.25% trypsin (Gibco) for further subculturing. Cells from passage three (P3) to passage five (P5) were used in this study to avoid functional changes due to the longtime culture.

Cell proliferative activity: HDPSCs were seeded into 96-well plates at a density of 5×10^3 cells/well and cultured until indicated time points (1 d, 2 d, 3 d, 4 d, 5 d, 6 d, and 7 d). The original medium was replaced with 100 μl/well fresh medium and 10 μl/well Cell Counting Kit-8 (CCK-8) reagent (Boster, Wuhan, China) and kept in dark conditions for 1 hr. at 37°C. The cell viability was determined by measuring the absorbance at 450 nm using a Thermo Scientific microplate absorbance reader (Shanghai, China).

Flow cytometric analysis of cell phenotype: For identification of cell phenotype, 1×10^6 hDPSCs were collected and washed twice with cold PBS containing 0.1% BSA, and then incubated with phycoerythrin (PE) conjugated antibodies: 20 μl STRO1, 20 μl CD45, 20 μl CD29, 10 μl CD34 (BD, USA), or fluorescein isothiocyanate (FITC) conjugated antibodies: 5 μl CD146, 20 μl CD44, 3 μl CD90, PE or FITC-conjugated nonspecific mouse IgG1 (BD, USA) as a negative control for 30 min at 4°C. The cells were washed with cold PBS to remove unconjugated antibodies and resuspended with 500 μl PBS. Then the labeled cells were analyzed using a flow cytometer (BD Biosciences, San Jose, CA, USA) [29].

Osteogenic differentiation of stem cells and the Alizarin red S assay: The cells were seeded into 6-well plates and cultured until 70% confluence. For osteogenesis, the osteogenic/odontogenic differentiation medium was the growth medium supplemented with 50 μM ascorbic acid 2 phosphate (Sigma-Aldrich, USA), 10 mM β glycerophosphate (Sigma-Aldrich, USA), and 100 nM dexamethasone (Sigma-Aldrich, USA). After incubated with osteogenic/odontogenic differentiation medium and cultured for 3 weeks to induce mineral formation, the cells were fixed with 4% paraformaldehyde for 30 min, stained with 40 mM alizarin red S (pH 4.0, Sigma-Aldrich, USA) for 30 min at room temperature, and then photographed using a digital camera (Nikon, Japan) and Olympus FSX100 microscope (Olympus Corporation, Tokyo, Japan) for qualitative evaluation of mineralizing nodules. For quantification, the calcium nodules were fully dissolved with 10% acetic acid (500 μl/well) for 30 min at 37°C. After collection, the supernatant, the acid in which was neutralized with 75 μl 10% ammonium hydroxide, and ARS standards were added (150 μl/well) into a 96-well plate in triplicate. A microplate reader was employed to read the absorbance at 405 nm. In the meantime, an ARS standard curve was plotted to calculate the ARS concentration of each sample.

Adipogenic differentiation of stem cells: The HDPSCs adipogenic differentiation medium kit (HUXDP-90031, Cyagen, Suzhou, China) was employed for adipogenesis according to the manufacturer's instructions. Cells were first cultured in the induction medium (A solution: basal medium A supplemented with 10% FBS, 1% penicillin-streptomycin, 1% glutamine, 0.2% insulin, 0.1% 3-isobuty-1-methylxanthine

(IBMX), 0.1% rosiglitazone, and 0.1% dexamethasone) for 3 days. Cells were then incubated with maintenance medium (B solution: basal medium B supplemented with 10% FBS, 1% penicillin-streptomycin, 1% glutamine, and 0.2% insulin) for 1 day. Then the medium was changed back to induction medium. After 5 times (20 days) of alternating cultivation between A solution and B solution, cells were maintained in B solution for 7 days until the lipid droplets grew big enough. The cells were fixed in 4% paraformaldehyde for 30 min and stained with 2% fresh oil-O red solution for 30 min. The lipid area was recorded with an Olympus FSX100 microscope.

Loading conditions for mechanical stress

Mechanical stress stimulation loading device: The experimental apparatus used in our study was devised by researchers in the Key Laboratory of Shaanxi Province for Craniofacial Precision Medicine Research, College of Stomatology, XJTU, Shaanxi, China. The pressure loading on cells was precisely controllable. HDPSCs (2×10^5 cells/well) were seeded into 6-well plates and cultured for 70% confluence. Cells in osteogenic/odontogenic differentiation medium were exposed to mechanical stress (control, 0.09 MPa, and 0.18 MPa) for 30 minutes per day. The culture medium was changed every three days.

Annexin V-FITC/PI apoptosis analysis: At indicated time points (1 d and 3 d), all cells suspended in medium and adhered to the bottom of plates were harvested. The apoptotic rate was determined by Annexin V-FITC/PI double staining cell apoptosis detection kit (7 sea biotech, Shanghai, China) according to the manufacturer's instructions. Cells were resuspended in 1×binding buffer and incubated with 5 μl Annexin V-FITC at room temperature out of light for 15 minutes. Then, 10 μl PI reagent was added into test tubes and fully mixed with cells. Cell apoptotic rates were measured using a flow cytometer.

Alkaline Phosphatase (ALP) staining: The BCIP/NBT Alkaline Phosphatase Staining Kit (Beyotime, Shanghai, China) was used to qualitatively evaluate the effects of mechanical stress on the intracellular ALP activity of hDPSCs according to the manufacturer's instructions. After exposure to mechanical stress (0.09 Mpa and 0.18 Mpa) in osteogenic/odontogenic differentiation medium for 7 days and 14 days, respectively, hDPSCs were fixed with 4% paraformaldehyde for 30 min, stained with ALP staining working solution for 10 min at room temperature, and then photographed under a digital camera and Olympus FSX100 microscope for qualitative evaluation. The average optical density measured by ImageJ of each sample was evaluated for semi-quantification.

Western blot (WB) analysis: Cells were washed in cold PBS and total proteins were extracted in RIPA lysis buffer supplemented with PMSF and protease inhibitor cocktail (Roche, Switzerland). Crude lysates were centrifuged at 13000 rpm for 10 min. The supernatant was collected, and protein concentration was measured using BCA assays (Boster, Wuhan, China). Protein was fractionated by 8%, 10%, and 15% SDS-PAGE, respectively. Proteins were transferred to PVDF membranes and blocked in 5% non-fat milk. Membranes were probed overnight with primary antibodies at 4°C, then washed, and labeled with the appropriate secondary antibodies. Anti-DSPP antibody (bs-10316R, Bioss, 1:500 dilution), anti-DMP1 antibody (bs-12359R, Bioss, 1:500 dilution), anti-RUNX2 antibody (ab23981, Abcam, 1:1000 dilution), anti-GAPDH antibody (bs-12257R, Bioss, 1:5000 dilution), and Goat Anti-Rabbit IgG Secondary Antibody (BA1054, Bioss, 1:2000 dilution) were used for immunoblot assays. The immunereactive bands were visualized using enhanced chemiluminescent reagents. The original western blot membranes corresponding with the representative images are present in Figure S1.

MiRNA array and data analysis

Biochip detection was performed by GENECHIEM (Shanghai, China). Briefly, as follows.

Sample preparation: HDPSCs in osteogenic/odontogenic differentiation medium were exposed to mechanical stress (0.09 MPa, 30 min/d, for 7 days). Total RNA was extracted with Trizol Reagents (Takara, Japan). A260/A280 value and RIN value of the RNA were measured using Nanodrop (Thremo Nanodrop 2000) and Agilent RNA 6000 Nano Kit (Agilent 2100 Bioanalyzer), respectively. Quality control standards of RNA was $1.7<A260/A280<2.2$, RIN ≥7.0, and $28S/18S>0.7$.

MiRNA GeneChip: The FlashTag™ Biotin HSR RNA Labeling Kit and GeneChip miRNA 4.0

Table 1. The expression of 8 differentially expressed miRNAs in mechanical stressed hDPSCs

MiRNA	FC	logFC	*P* Value	Regulated
Hsa-miR-30e-5p	2.956605314	1.56394166666667	0.0335223531490189	Up
Hsa-miR-154-3p	2.655223556	1.40883333333333	0.00913494247510589	Up
Hsa-miR-134-3p	2.250231348	1.17007333333333	0.00262415715219882	Up
Hsa-miR-19a-3p	2.078731369	1.05570333333333	0.0180515994843644	Up
hsa-miR-431-3p	2.018672211	1.01340666666667	0.0118378118040979	Up
Hsa-miR-6165	-2.218836454	-1.14980333333333	0.0165946165451668	Down
Hsa-miR-6831-5p	-2.113362133	-1.07954	0.0298754833763258	Down
hsa-miR-4442	-2.04038302	-1.02884	0.00315233459875951	Down

Note: Fold change (FC) is a measure describing how much a quantity changes going from an initial to a final value. The Log fold-change (logFC) is an estimate of the log ratio of expression in a cluster to that in all other cells. A value of 1.0 indicates a 2-fold higher expression in the cluster of interest.

Table 2. The primer sequences for specific reverse transcription polymerase chain reaction of miRNAs

Genes	Reverse transcription primer sequence (5'–3')
U6	CGCTTCACGAATTTGCGTGTCAT
Hsa-miR-30e-5p	GTCGTATCCAGTGCGTGTCGTGGAGTCGGCAATTGCACTGGATACGACCTTCCAG
Hsa-miR-154-3p	GTCGTATCCAGTGCGTGTCGTGGAGTCGGCAATTGCACTGGATACGACAATAGGT
Hsa-miR-134-3p	GTCGTATCCAGTGCGTGTCGTGGAGTCGGCAATTGCACTGGATACGACTTGGTGA
Hsa-miR-19a-3p	GTCGTATCCAGTGCGTGTCGTGGAGTCGGCAATTGCACTGGATACGACTCAGTTT
Hsa-miR-6165	GTCGTATCCAGTGCGTGTCGTGGAGTCGGCAATTGCACTGGATACGACCTCCCCT
Hsa-miR-6831-5p	GTCGTATCCAGTGCGTGTCGTGGAGTCGGCAATTGCACTGGATACGACGACCTCC

were used to detect the miRNA expression profiles. The RNA was tailed and labeled with Poly(A) and biotin, respectively. The RNA samples were treated with GeneChip hybridization and stain reagents (GeneChip Hybridization Oven 645 and GeneChip Fluidics Station 450). GeneChips were scanned to collect raw data (GeneChip Scanner 3000).

Bioinformatics: Differentially expressed microRNAs were selected according to *P*-value <0.05 and fold change (FC) >2 or FC<-2. Putative target genes of these microRNAs were predicted in seven databases, Targetscan, RNA22, PicTar, RITA, miRmap, miRanda, and microT. Protein-protein interactions (PPI) network was performed through STRING. GO terms and KEGG pathway were further analyzed to identify gene and biological pathway enrichment. The *P*-value indicates the importance of the path related to the condition (the recommended critical *P*-value was 0.05) [30-32].

Quantitative real-time polymerase chain reaction (qRT-PCR): The qRT-PCR was performed to validate miRNA sequencing data. Total RNA was extracted with TRIzol Reagent and then converted to synthesize cDNA using Prime Script® RT Reagent Kits (Takara, Japan) under the conditions of 42°C for 15 min, 85°C for 5 s, and 4°C for 15 min. QRT-PCRs were performed to amplify cDNA with SYBR Green PCR Master Mix kits (Takara, Japan). The reaction conditions were conducted according to the manufacturer's instructions in an ABI 7500 Real-Time PCR system (Applied Biosystems, Singapore). The sequences of reverse transcription polymerase chain reaction primers and quantitative real-time polymerase chain reaction primers used in the present study are shown in **Tables 2**, **3**, and S1, respectively. The gene expression was normalized to U6 and calculated using the $2^{-\Delta\Delta Ct}$ method [33].

Statistical analysis

Data were represented as mean ± standard error. All data were statistically and graphically analyzed using GraphPad Prism 6.0 software. Students' t-test were used for comparison between groups and the actual statistical analysis method for each analysis is presented in Table S2. The *P*-value less than 0.05 was considered significant.

Table 3. The primer sequences for specific quantitative real-time polymerase chain reaction

Genes	Primers	Primer sequence (5'---3')
Hsa-U6	Forward	CTCGCTTCGGCAGCACA
Hsa-U6	Reverse	AACGCTTCACGAATTTGCGT
Hsa-miR-F	Common forward primer	ATCCAGTGCGTGTCGTG
Has-miR-30e-5p	Reverse	TGCTTGTAAACATCCTTGA
Hsa-miR-154-3p	Reverse	TGCTAATCATACACGGTTG
Hsa-miR-134-3p	Reverse	TGCTCCTGTGGGCCACCTAG
Has-miR-19a-3p	Reverse	TGCTTGTGCAAATCTATGCA
Hsa-miR-6165	Reverse	TGCTCAGCAGGAGGTG
Hsa-miR-6831-5p	Reverse	TGCTTAGGTAGAGTGTGAGGA

Results

HDPSCs isolation and identification

HDPSCs derived from dental pulp explants were isolated with the method of tissue-enzymatic digestion and cultured in growth medium. The isolated cells were monitored under a light microscope daily. The experiments were started when the cells crawled out from the tissue masses and became spiral and clumped confluences (**Figure 1Aa-c**). The cell vitality was checked using CCK-8 test kits. Cells in the S-shaped growth curve and P3 to P5 were used in all experiments in the present study (**Figure 1B**). To characterize the hDPSCs, we performed flow cytometry experiments using specific surface markers for hDPSCs. Cells which were positive for the markers of mesenchymal stem cell (MSC), CD29, CD44, CD90, CD105, CD146, and STRO1 (**Figure 1Cd**, **1Ce**, and **1Cg-j**) and negative for the markers of hematopoietic stem cells, CD34, and CD45 (**Figure 1Cb**, **1Cc**) were classified as DPSCs. It is known that DPSCs are osteogenic/odontogenic and adipogenic upon different induction. To further characterize the cells, we stained the cells with Alizarin red S (ARS) and found clearly that the ARS intensity was significantly increased in the cells cultured in osteogenic/odontogenic differentiation medium at week 3 (**Figure 1Ae**, **1Af**) comparing to control (**Figure 1Ad**). The calcified nodules and calcium phosphate crystals secreted from hDPSCs during osteogenesis/odontogenesis, were observed in these cell cultures (**Figure 1Ae**, **1Af**). We cultured the hDPSCs in adipogenic differentiation medium and checked the adipogenesis with oil-O red staining. The results showed significant lipid droplets of oil-O red in these cell cultures at week 4 (**Figure 1Ah**, **1Ai**) comparing to control (**Figure 1Ag**), suggesting a differentiation from hDPSCs into adipocytes. Taken all these data together, we demonstrated that the isolated hDPSCs were pluripotent cells that can differentiate into osteogenesis and adipogenesis.

The impact of mechanical stress on the proliferation and apoptosis of hDPSCs

To determine the effects of mechanical stress on the proliferation of hDPSCs, we performed a cell vitality test using the CCK-8 kits, and found that both mechanical stress, 0.09 MPa, and 0.18 MPa, can significantly promote the proliferation of hDPSCs starting on day 5 till day 7 comparing to the controls, no significant difference was observed before day 5 (**Figure 2A**). This impact on the proliferation of hDPSCs was independent of the strength of the mechanical stress applied to the cells (**Figure 2A**). To exclude the physical damage caused by the mechanical stress, the cultured DPSCs were exposed to 0.09 MPa and 0.18 MPa mechanical stresses, respectively, for one day and three days. The cell apoptosis was determined by flow cytometry. The results indicated that there was no significant difference between mechanic-stressed cells and control cells (no stress applied) (**Figure 2B**). These data demonstrated that the mechanical stress did not physically cause damage to hDPSCs, but promoted the proliferation of these cells.

Alkaline phosphatase activity and extracellular matrix mineralization of hDPSCs in response to mechanical stress

It has been shown that mechanical stress plays an important role in the proliferation and osteo/odontoblastic differentiation of odontogenic MSCs [17, 34]. To study the differentially expressed miRNAs during osteogenic/odontogenic differentiation of hDPSCs under the condition of mechanical stress, we verified if the mechanical stress could induce the osteogenic/odontogenic differentiation of hDPSCs under the conditional medium. HDPSCs in osteogenic/odontogenic differentiation medium were exposed to two different mechanical stimulations, 0.09 MPa, and 0.18 MPa, for 7 days and 14 days, respectively. The osteogenic/odontogenic differentiation was verified with ALP and

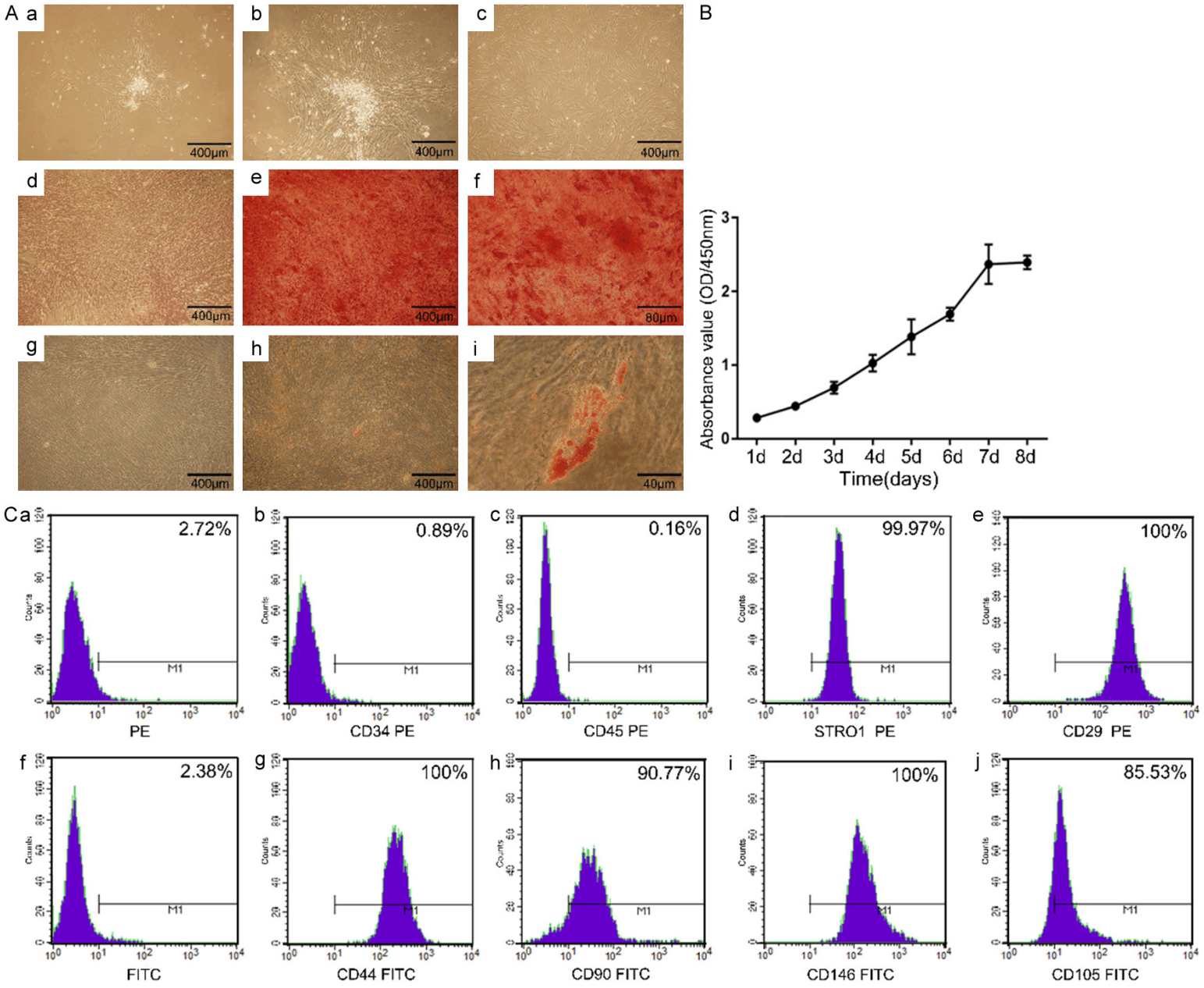
A a
b
c
400μm
d
e
f
80μm
g
h
i
40μm
B
Absorbance value (OD/450nm)
Time(days)
1d 2d 3d 4d 5d 6d 7d 8d
Ca
2.72%
PE
0.89%
CD34 PE
0.16%
CD45 PE
99.97%
STRO1 PE
100%
CD29 PE
2.38%
FITC
100%
CD44 FITC
90.77%
CD90 FITC
100%
CD146 FITC
85.53%
CD105 FITC
M1
Counts

Figure 1. Characterization of hDPSCs. Aa, Ab. Primary cultured cells on the third day and seventh day. Ac. Sub-cultured hDPSCs cells. Ad. Negative control of osteogenic differentiation of hDPSCs stained by ARS. Ae, Af. Osteogenic differentiation of hDPSCs stained by ARS. Ag. Negative control of adipogenic differentiation of hDPSCs stained by oil-O red. Ah, Ai. Adipogenic differentiation of hDPSCs stained by oil-O red. Aa-e and Ag, Ah. Scale bar, 400 μm; Af. Scale bar, 80 μm; Ai. Scale bar, 40 μm. B. Growth curve of hDPSCs. C. The flow cytometry analysis of the specific surface markers of hDPSCs. Ca, Cf. Negative control of the PE-labeled and FITC-labeled surface markers. Cb, Cc. Surface markers of hematopoietic stem cells CD34 and CD45. Cd, Ce. Cg-j. Surface markers of mesenchymal stem cells STRO1, CD29, CD44, CD90, CD146, and CD105.

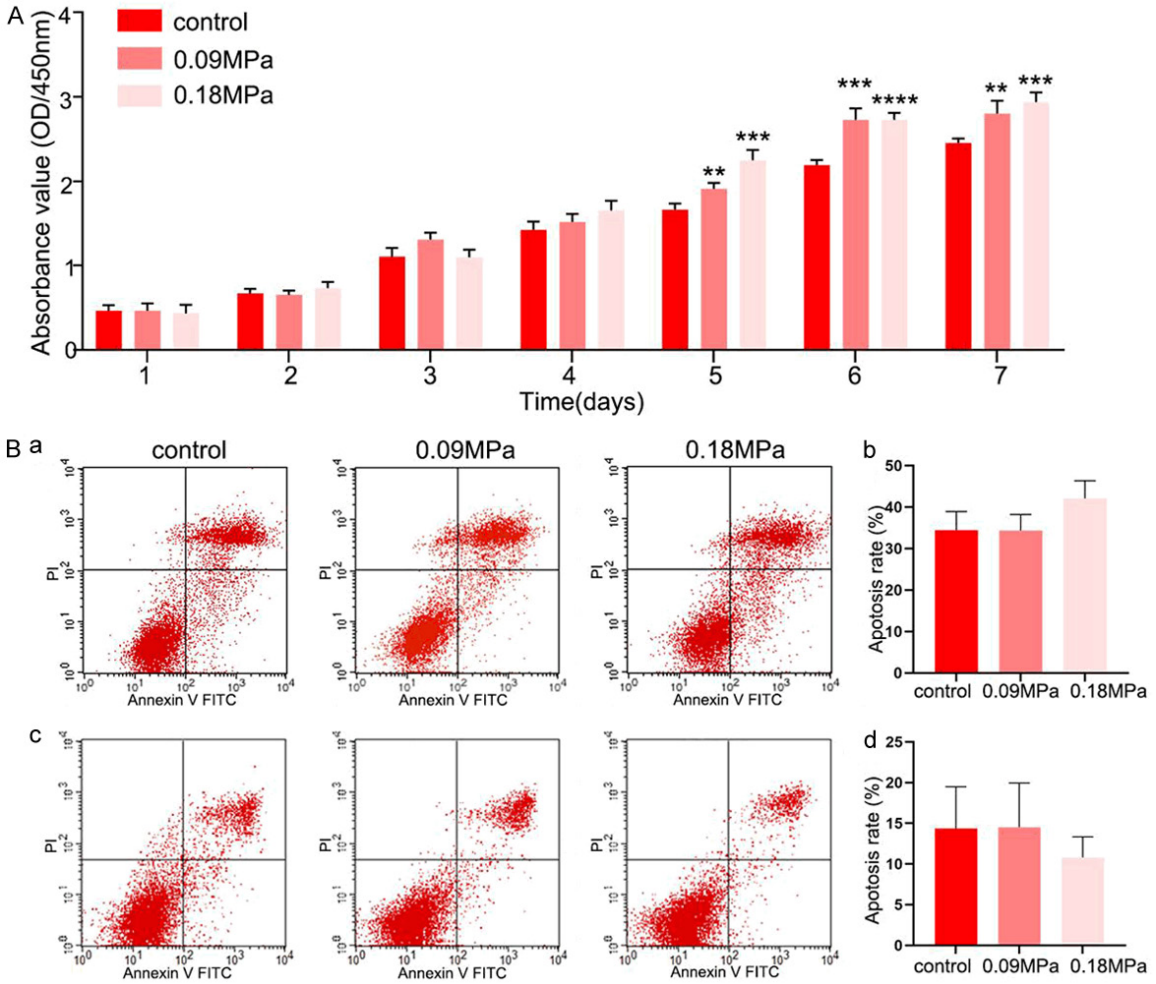

Figure 2. The effects of mechanical stress on the viability of hDPSCs. A. HDPSCs were treated with mechanical stress (control, 0.09 MPa, and 0.18 MPa), and cell proliferation was assessed using the CCK-8 assay (n=4). B. The flow cytometry analysis of apoptosis. Ba, Bc. Representative images of cell apoptosis of hDPSCs treated with mechanical stress for 1 day and 3 days. Bb, Bd. Quantitative analysis of cell apoptosis rate after mechanical stress treatment for 1 day and 3 days (n=3). Results were analyzed by Student's t-test. Data were presented as mean ± standard deviation. $^{**}P<0.01$, $^{***}P<0.001$, and $^{****}P<0.0001$ when comparing to control.

ARS staining. On day 7 after mechanical stress exposure, the ALP activity and calcium concentration in the mineralizing deposits of cultured hDPSCs in response to both mechanical stresses were significantly increased compared to the controls (**Figure 3Aa**, **3Ab**, **3Ba**, **3Bb**). On day 14, both mechanical stresses inhibited the osteogenic/odontogenic differentiation of hDPSCs as indicated by the ALP staining. ARS staining and the concentration of calcium in the mineralizing deposits. This inhibition was positively related with the volume of the mechanical stress applied (**Figure 3Ac**, **3Ad**, **3Bc**, **3Bd**). Our results showed that the mechanical stress regulated the osteogenic/odontogenic differentiation of hDPSCs in the earlier stage, but not in

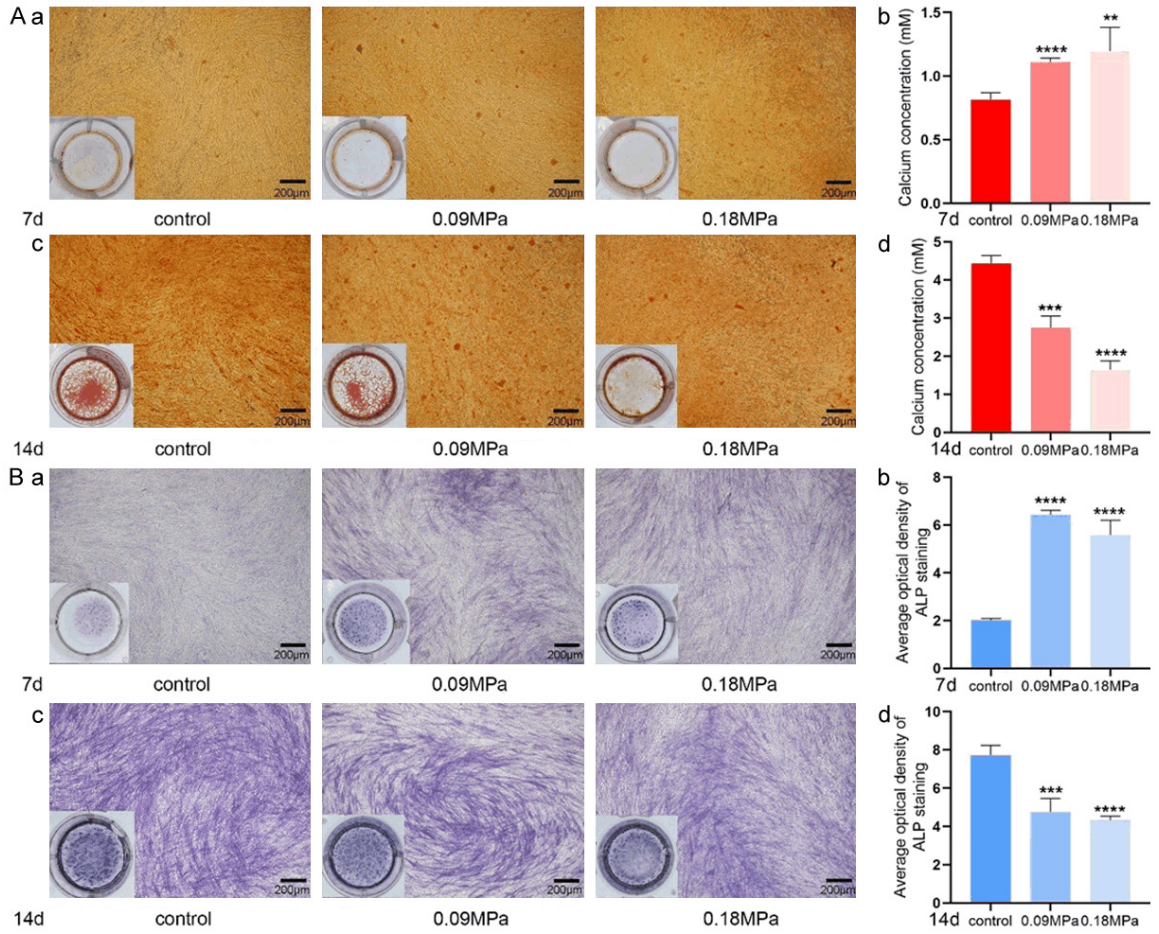

Figure 3. The effects of mechanical stress on the ALP staining and extracellular matrix mineralization in hDPSCs. A. The ARS staining and quantitative analysis of extracellular matrix mineralization. Aa. Representative images of ARS staining after 0.09 MPa and 0.18 MPa mechanical stress treatment for 7 days (n=4). Ab. Quantitative analysis of the calcium content in the mineralizing deposits after 0.09 MPa and 0.18 MPa mechanical stress treatment for 7 days (n=4). Ac. Representative images of ARS after 0.09 MPa and 0.18 MPa mechanical stress treatment for 14 days (n=4). Ad. Quantitative analysis of the calcium content in the mineralizing deposits after 0.09 MPa and 0.18 MPa mechanical stress treatment for 14 days (n=4). Scale bar, 200 μm. B. The ALP staining and semi-quantitative analysis of ALP staining. Ba. Representative images of ALP staining after 0.09 MPa and 0.18 MPa mechanical stress treatment for 7 days (n=4). Bb. Semi-quantitative analysis of ALP staining after 0.09 MPa and 0.18 MPa mechanical stress treatment for 7 days (n=4). Bc. Representative images of ALP staining after 0.09 MPa and 0.18 MPa mechanical stress treatment for 14 days (n=4). Bd. Semi-quantitative analysis of ALP staining after 0.09 MPa and 0.18 MPa mechanical stress treatment for 14 days (n=4). Results were analyzed by unpaired Student's t-test. Data are presented as mean ± standard deviation. Scale bar, 200 μm. $^{**}P<0.01$, $^{***}P<0.001$, and $^{****}P<0.0001$ when comparing to control.

the late stage. We chose the samples from 7-day stress exposure for the miRNA screening experiments.

The effects of mechanical stress on the expression of DSPP, DMP1, and RUNX2 of hDPSCs

To determine the effects of mechanical stress on the osteogenic/odontogenic differentiation of hDPSCs, we conducted WB experiments to check the expression levels of the biomarker proteins, DSPP, DMP1, and RUNX2. HDPSCs were cultured in osteogenic/odontogenic differentiation medium and exposed to 0.09 MPa and 0.18 MPa mechanical stress for 7 and 14 days, respectively. On day 7, the expression of DSPP, DMP1, and RUNX2 were evaluated upon the application of 0.09 MPa and 0.18 MPa mechanical stress compared to the control group. No difference was observed between the mechanical stress groups (**Figure 4A**).

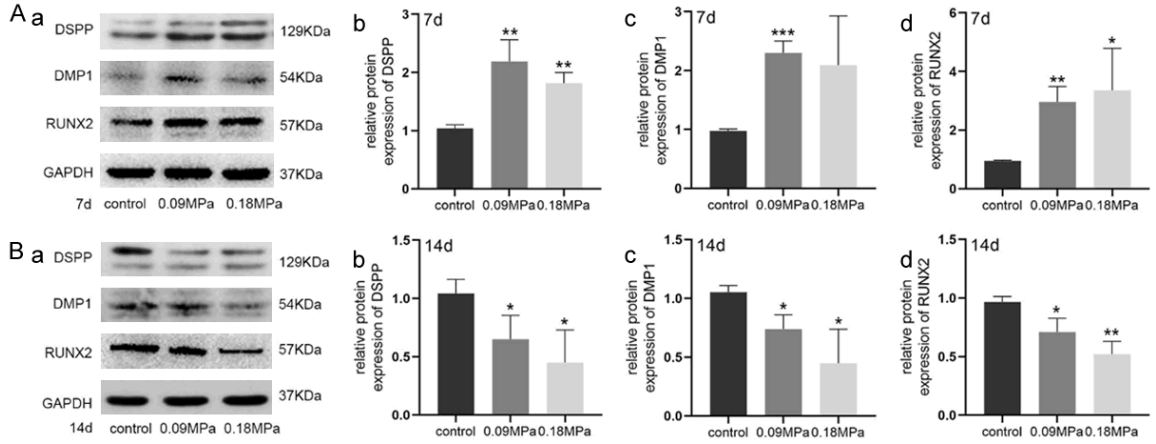

Figure 4. The relative expression levels of DSPP, DMP1, and RUNX2 after treatment with mechanical stress for 7 days and 14 days. A. The relative expression levels and semi-quantitative analysis of DSPP, DMP1, and RUNX2 in hDPSCs treated with mechanical stress for 7 days. Aa. Representative western blot scans of each protein in hDPSCs treated with 0.09 MPa and 0.18 MPa mechanical stress for 7 days. Ab-d. Semi-quantitative analysis of the relative protein expression levels in hDPSCs treated with 0.09 MPa and 0.18 MPa mechanical stress for 7 days (n=3). B. The relative expression levels and semi-quantitative analysis of DSPP, DMP1, and RUNX2 in hDPSCs treated with mechanical stress for 14 days. Ba. Representative western blot scans of each protein in hDPSCs treated with 0.09 MPa and 0.18 MPa mechanical stress for 14 days. Bb-d. Semi-quantitative analysis of the relative protein expression levels in hDPSCs treated with 0.09 MPa and 0.18 MPa mechanical stress for 14 days (n=3). Results were analyzed by unpaired Student's t-test. Data are presented as mean ± standard deviation. *P<0.05, **P<0.01, and ***P<0.001 when comparing to control.

When the hDPSCs were mechanically stressed (0.09 MPa and 0.18 MPa) for 14 days, the expression level of DSPP, DMP1, and RUNX2 were decreased compared to the control groups (**Figure 4B**). These data, in line with the ALP and ARS staining, suggested that mechanical stress can upregulate the expression of DSPP, DMP1, and RUNX2 in the earlier time of the stress (7 days), but inhibited their expression in the late stage (14 days).

Differential expression of miRNAs in hDPSCs in response to the mechanical stress

We performed miRNA array analysis between the mechanically stressed hDPSCs and unstressed hDPSCs (control). The mechanical stress applied here was 0.09 MPa (30 min/day) for 7 days. The volcano plot and heat map showed the varied miRNA expressions between the mechanical stress group and the control group (**Figure 5A**, **5B**). We identified 8 differentially expressed miRNAs in the mechanically stressed hDPSCs compared to the control. Of these 8 miRNAs, 5 miRNAs were significantly upregulated and 3 miRNAs were significantly downregulated (P<0.05, FC>2 or <-2). The fold change of these miRNAs is exhibited in **Table 1**. To validate the results, we conducted qRT-PCR analysis on six miRNAs (hsa-miR-30e-5p, hsa-miR-154-3p, hsa-miR-134-3p, hsa-miR-19a-3p, hsa-miR-6165, and hsa-miR-6831-5p), and found that hsa-miR-30e-5p, hsa-miR-154-3p, hsa-miR-134-3p, and hsa-miR-19a-3p were significantly upregulated in the mechanically stressed hDPSCs compared to the unstressed hDPSCs (**Figure 5C**). The qRT-PCR data confirmed the downregulated expression of hsa-miR-6165 and hsa-miR-6831-5p with significant difference between the stressed group and unstressed group (**Figure 5C**). The expression of the differentially expressed miRNAs after prolonged exposure was analyzed and showed in Figure S2A and S2B.

Bioinformatics of PPI-network and functional enrichment

To predict the putative target genes of miRNAs, we run through 7 different databases: Targetscan, RNA22, PicTar, miRmap, and microT. Only those target genes which appeared in at least 4 databases were considered as the putative target genes of the particular miRNAs. Based on this criterion, our results showed that only 3 upregulated miRNAs, hsa-miR-30e-5p, hsa-miR-19a-3p, and hsa-miR-154-3p, fulfilled this criterion and gave a total of 1668 pairs found in the target gene prediction (**Figure 6A**). The protein-protein interaction (PPI) network was calculated using STRING. Only the interac-

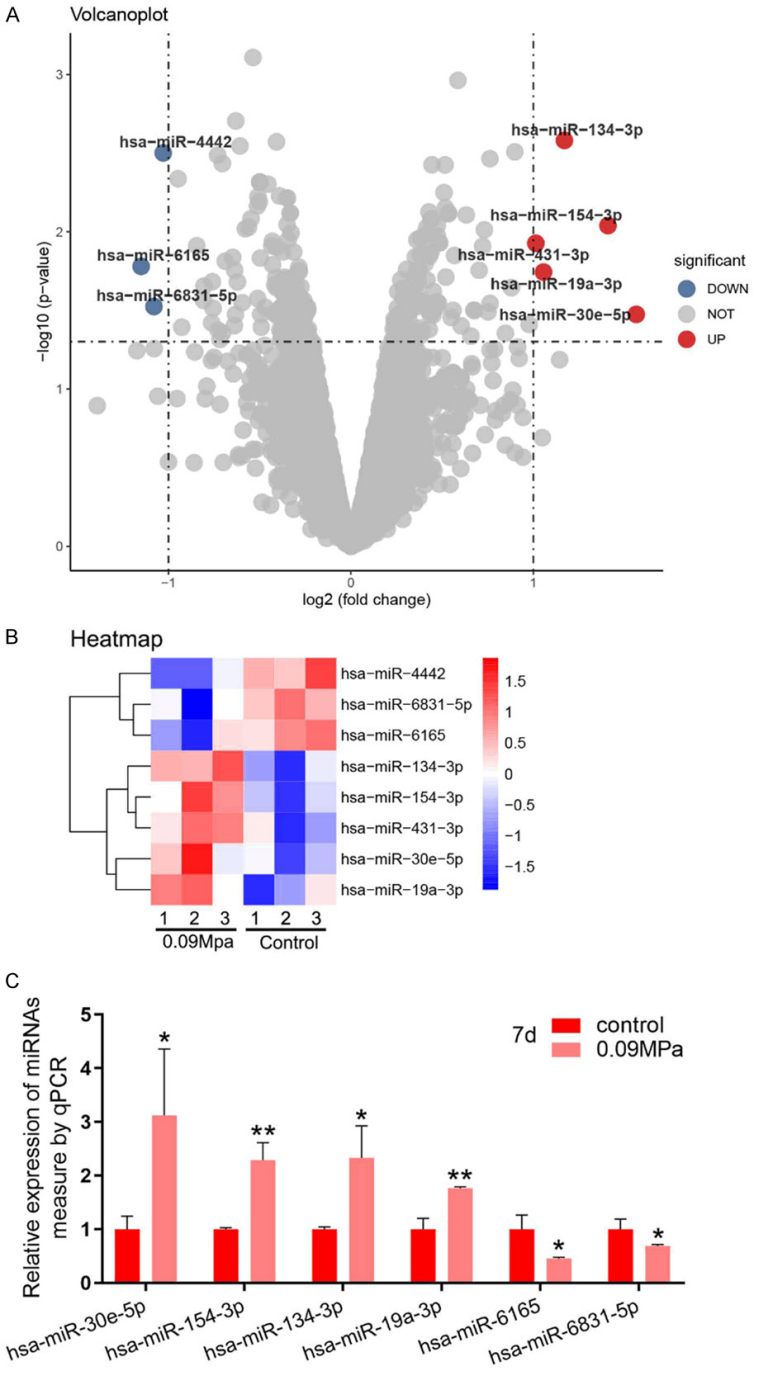

Figure 5. The microarray profiles of differentially expressed miRNAs during the osteogenic/odontogenic differentiation of hDPSCs with or without mechanical stress. A. Volcano map of differentially expressed miRNAs. The volcano map reflected the number, significance, and reliability of differentially expressed miRNAs. Axis represents log2-scaled fold changes and *P*-values (-log10 scaled). Vertical-dotted lines represent ≥2.0× fold change, whilst horizontal-dotted lines represent *P* values less than 0.05. Red and blue dots signify up- and downregulated miRNAs, respectively. B. Heatmap of differentially expressed miRNAs. Screening criteria were fold change >2 and P<0.05. The expression value is described by color scale. The intensity increased from blue to red. Each column represents one sample, and each row represents one transcript. C. Relative expression of miRNAs normalized to U6. Results were analyzed by unpaired Student's t-test. Data are presented as mean ± standard deviation. *P<0.05 and **P<0.01 when comparing to control.

tion scored greater than 0.4 were exhibited in the network (**Figure 6B**), which included 101 nodes and 146 edges. According to the gene expression, the top 5% genes were selected as hub genes, KRAS, SIRT1, SOCS3, KLHL20, RAP1B, and CBFB. Also the mRNA expression of those hub genes were further analyzed in the hDPSCs treated with 0.09 MPa mechanical stress for 7 days (Figure S2C). The target genes belonging to the same subset in the PPI network were a module or sub-network. Only one sub-network was clustered in the Cluster page of STRING (**Figure 6C**).

Gene ontology (GO) analysis was performed to predict the functional enrichment of target genes. The top 20 GO terms are listed in **Figure 7Aa**, **7Ab**, including epithelial cell development, Rap protein signal transduction, the establishment of endothelial barrier, endothelium development, and modification by symbiont of host morphology or physiology, and cellular response to external stimulus.

Kyoto Encyclopedia of Genes and Genomes (KEGG) pathway analysis was used to predict the signaling pathway enrichment of target genes. The top 20 signaling pathways are shown in **Figure 7Ba**, **7Bb**. These enriched signal pathways included Rap1, regulation of actin cytoskeleton, cAMP, MAPK, Neurotrophin, growth hormone synthesis, secretion, action, and Gap junction.

Discussion

Dental pulp stem cells play important roles in dental and dental pulp regeneration [1].

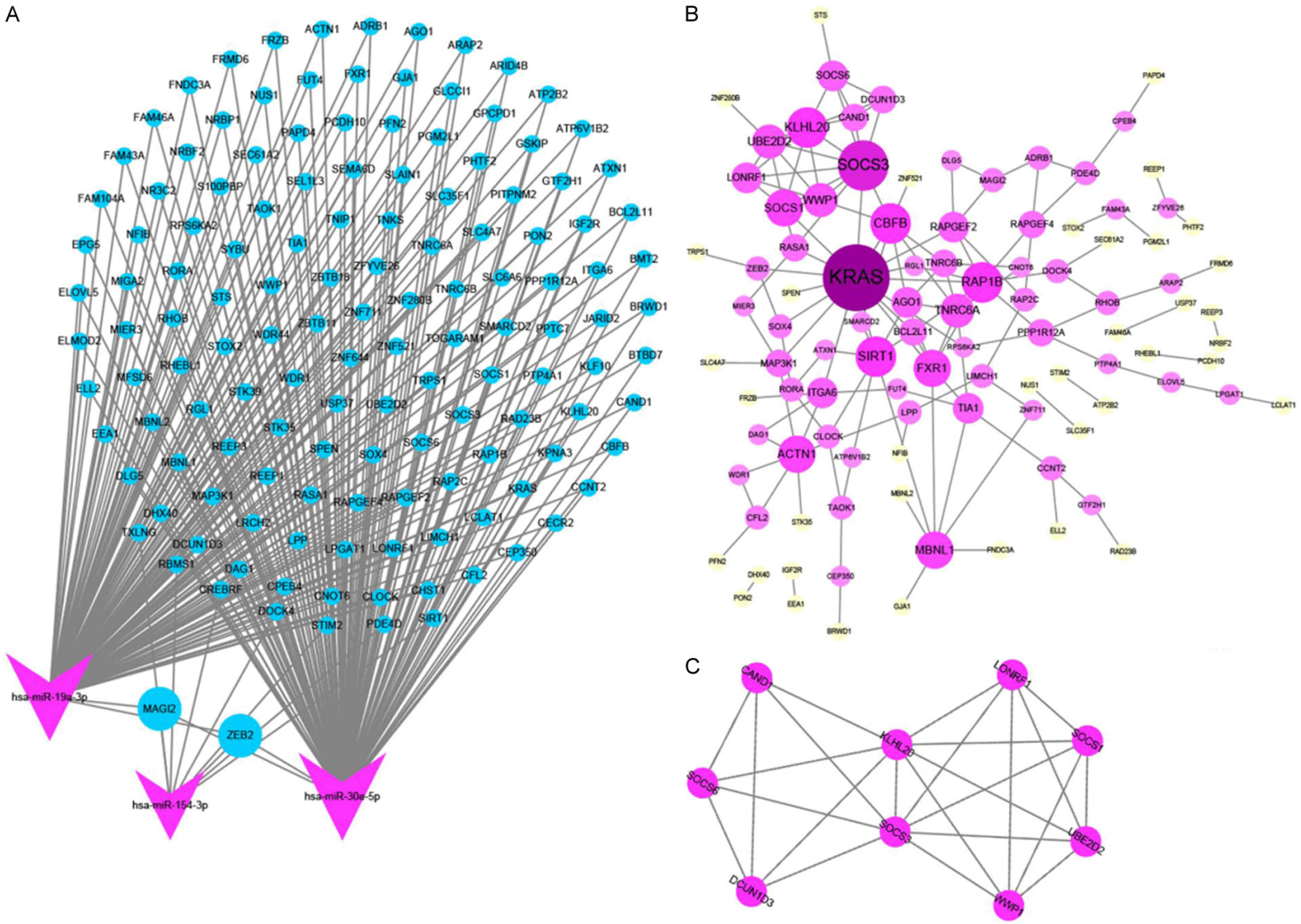

Figure 6. The prediction of target genes of differentially expressed miRNAs and protein-protein interaction network. A. The prediction of target genes of differentially expressed miRNAs was performed in seven databases (Targetscan, RNA22, PicTar, RITA, miRmap, miRanda, and microT). Target genes that appeared in no less than four databases were selected. B. Protein-protein interaction (PPI) network was calculated in STRING, from which interaction scored more than 0.4 was chosen. Each node represented a kind of protein and each edge represented some kind of interaction between them. C. PPI network cluster.

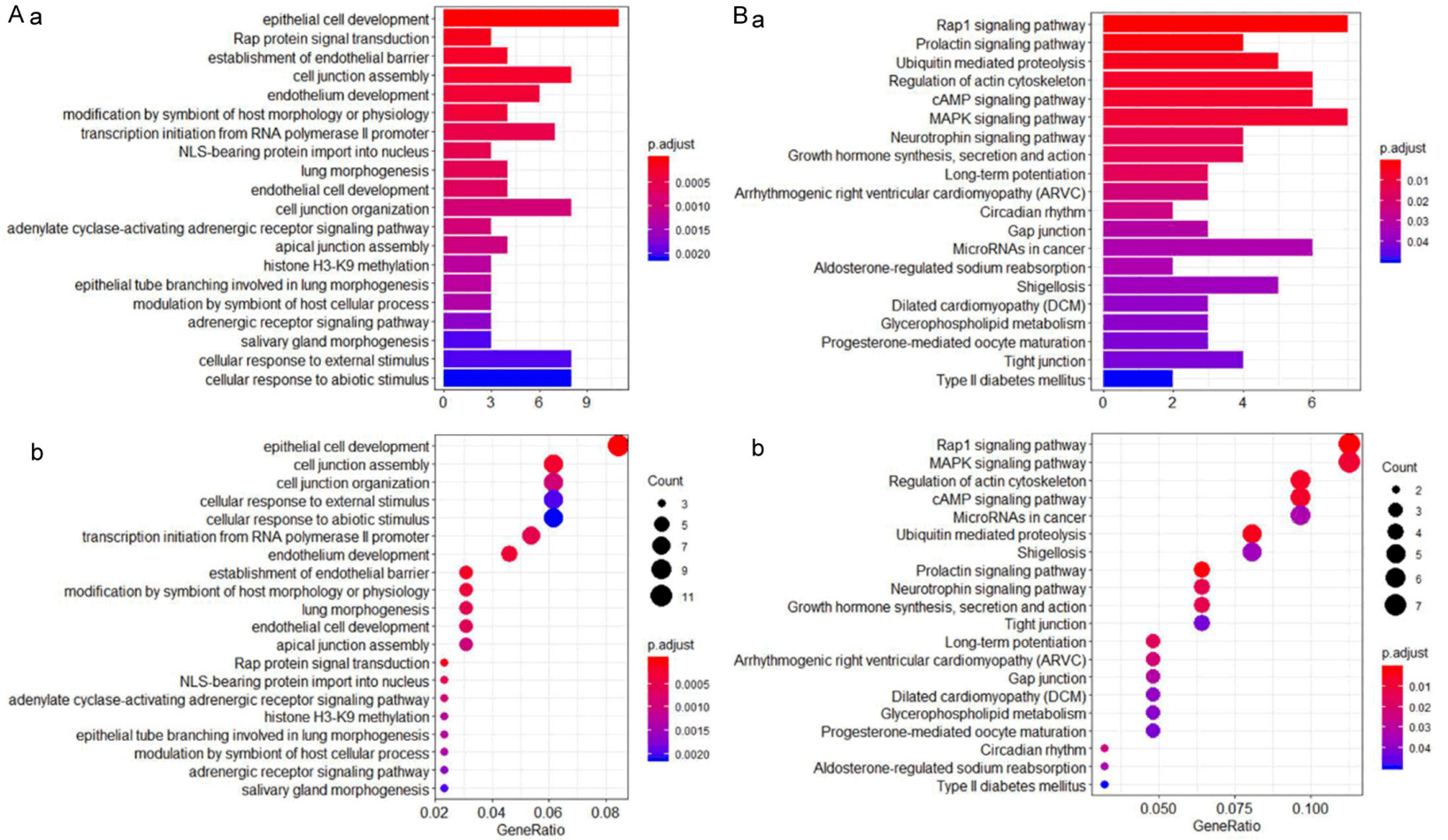

Figure 7. The enrichment analysis of target genes of differentially expressed miRNAs. GO biological process enrichment and KEGG pathway enrichment were analyzed in GEO bioinformatics (P<0.05). A. GO biological process enrichment. Aa. The top 20 significant GO biological processes of target genes of differentially expressed miRNAs presented with bar charts. Ab. The top 20 significant GO biological processes of target genes of differentially expressed miRNAs presented with bubble charts. B. KEGG pathways enrichment. Ba. The top 20 significant KEGG pathway of target genes of differentially expressed miRNAs presented with bar charts. Bb. The top 20 significant KEGG pathways of target genes of differentially expressed miRNAs presented with bubble charts. Gene Ratio represented the ratio of genes located in the GO biological process enrichment and KEGG pathway enrichment. Increased Gene Ratios indicated higher enrichment while count referred to gene number. The *P*-value was adjusted after multiple hypothesis test corrections, the smaller of which represented the greater significance. GO, Gene Ontology; KEGG, Kyoto Encyclopedia of Genes and Genomes; cAMP, cyclic adenosine monophosphate; MAPK, Mitogen Activated Protein Kinases.

Due to their mechanosensitive feature, these cells can recognize mechanical changes in the microenvironment around them and transform this information into cellular responses [35]. Several studies have demonstrated that different mechanical stimuli, such as cyclic mechanical tension, low-intensity pulsed ultrasound, and cyclic uniaxial compressive stress can significantly promote the proliferation of DPSCs *in vitro* [18, 36-38]. In the present study, we showed that mechanical stress can significantly increase the proliferation/self-renewal and osteogenic/odontogenic differentiation of hDPSCs by day 7. Utilizing the miRNA array analysis, we bioinformatically identified eight differentially expressed miRNAs during osteogenic/odontogenic differentiation of hDPSCs in response to mechanical stress. Of them, five miRNAs were upregulated, and three miRNAs were downregulated.

Like other mesenchymal stem cells, DPSCs reside in a niche consisting of an extracellular matrix, other local cell types, and biochemical stimuli [10]. These microenvironmental factors can influence the fate of DPSCs in terms of self-renewal/proliferation or differentiation. Previous studies have demonstrated that some mechanical stimuli can increase the proliferation of DPSCs [18, 39-41]. Other mechanic stimulation such as dynamic hydrostatic pressure can decrease DPSCs' vitality, even resulting in cell apoptosis [16], indicating that different mechanical stimuli could influence the decision between the DPSC proliferation/self-renewal and differentiation. It has been shown that a few mechanical stimuli have a dual function: positively regulating the proliferation of DPSCs and negatively regulating the differentiation of DPSCs, for instance, uniaxial mechanical stretch [18]. Here we reported that mechanical stress was promoting the proliferation/self-renewal and osteogenic differentiation of hDPSCs in earlier stage (up to 7 days). This inhibits the osteogenic/odontogenic differentiation of hDPSCs in later stage (from 7 days to 14 days).

Previous studies showed that miRNAs play an important role in the osteogenic/odontogenic differentiation of DPSC [25, 26]. In the present study, a total of 8 differentially expressed miRNAs were identified during the osteogenic/odontogenic differentiation of hDPSCs induced by mechanical stress. Of them, 5 miRNAs (hsa-miR-30e-5p, hsa-miR-154-3p, hsa-miR-134-3p, hsa-miR-19a-3p, and hsa-miR-431-3p) were significantly upregulated, and 3 miRNAs were significantly downregulated, which were all confirmed by qPCR. Hsa-miR-19a-3p has been shown to be upregulated in induced pluripotent stem cells from hDPSCs compared to hDPSCs. This indicated that hsa-miR-19a-3p may be involved in the differentiation of hDPSCs [42], which is in line with what we observed in the present study. hsa-miR-19a-3p was demonstrated to play roles in metastasis and proliferation of various tumor cells [43, 44]. The roles of hsa-miR-30e-5p were revealed in different types of cancers. It suppressed the angiogenesis and metastasis of squamous cell carcinoma of the head and neck [45], the proliferation and metastasis of nasopharyngeal carcinoma cells [46], and the tumorigenesis of non-small cell lung cancer [47]. A recent study has shown that hsa-miR-154-3p, together with miRNA-487-3p, synergistically inhibited the proliferation of thyroid cancer [48]. hsa-miR-134-3p has been demonstrated to have key roles in mediating the proliferation and cell cycle of human ovarian cancer stem cells [49]. For the significantly downregulated miRNAs, the studies from Dr. Mowla's lab have shown that hsa-miR-6165 was involved in neural apoptosis and differentiation. The overexpression of hsa-miR-6165 in the primary glioblastoma cell line (U87), promoted apoptosis by downregulating the predicated target genes (Pkd1 and DAGLA) [50]. When hsa-miR-6165 was overexpressed in the human pluripotent NT2 cell line, it can inhibit the neural differentiation of NT2 cells by downregulating the predicted target genes, like ABLIM-1, PVRL1, IGF-1R, and PDK1 target genes [51, 52]. We showed that, under the condition of differentiation of hDPSCs induced by the mechanical stress, the expression of hsa-miR-6165 was downregulated, and contributed to the differentiation of hDPSCs. Bioinformatic analysis of solid biopsies revealed that hsa-6831-5p was upregulated in metastatic samples of colorectal cancer compared to the non-metastatic samples [53]. In intramucosal carcinomas (IMCs) of stomach, hsa-miR-6831-5p was downregulated in metastatic IMC compared to nonmetastatic IMC [54], indicating that hsa-miR-6831-5p was involved in tumor metastasis in a tumor-type dependent manner. Our data showed that hsa-miR-6831-5p is linked to the differentiation of

hDPSCs. The exact biologic functions of these identified miRNAs in the differentiation of DPSCs need to be further investigated.

KRAS belongs to the RAS protein family which is responsible for cell proliferation and differentiation. The mutations in the KRAS gene are commonly found in human cancers, for example in ovarian cancer. It is associated with the differentiation of the cancer cells [55]. Fernandes et al. recently demonstrated that the expression level of KRAS was upregulated in the cancer stem cells of laryngeal cancer, one of the common head and neck tumors [56]. Another RAS protein family member, RAPIB, is also emerged as the predicted target. Recent studies have shown that Rap1b plays critical roles during skeletal development including chondrocyte and osteoblast differentiation [57]. It has been reported that miR-101-3p mediates the function of RAP1B in osteoclast differentiation [58].

In vitro and *in vivo* studies have shown that CBFB played critical roles in the differentiation of bone marrow mesenchymal stem cells and osteoblasts. Wu et al. showed that the deletion of CBFB promotes the adipogenic differentiation of bone marrow mesenchymal stem cells [59]. As a target of miR-145a, CBFB is essential for the osteogenic differentiation of MSCs negatively regulated by p53-induced miR-145a [60]. CBFB is a regulator of osteogenic differentiation. When the endogenous CBFB expression was decreased, the osteoblastic differentiation was halted [61].

SIRT1 mainly deacetylates its various targets, including histones, transcription factors, such as p53, NK-κB, and peroxisome proliferator-activated receptor γ (PPARγ), mediates the cell survival, differentiation, and bone metabolism [62]. Many studies have demonstrated that SIRT1 could balance bone formation and absorption by regulating the ratio of osteoblasts to osteoclasts [63, 64]. Evidence from *in vivo* and *in vitro* studies have revealed that SIRT played crucial roles in determining the fate of stem cells, such as SIRT1 can mediate the neuronal differentiation of neurons precursor cells [65], implicating its protection function of neurons from degeneration in neurological diseases. The activation of the SIRT1 with its activator, resveratrol, induces neuronal differentiation of two types of stem cells, the human bone marrow mesenchymal stem cells and human stem cells from apical papilla [66, 67]. Our data indicated that the specifically expressed miRNAs induced by the mechanical stress during the osteogenic/odontogenic differentiation of hDPSCs may regulate the fate of hDPSCs using these target molecules.

Bioinformatics analyses (GO and KEGG) were performed on these target genes to identify the regulated signaling pathway and biological processes. Several relevant pathways and processes have been identified, including epithelial cell development, cell junction assembly, cell junction organization, cellular response to an external stimulus, and cellular response to an abiotic stimulus. These are usually considered as “mechanosensors”, and the signaling pathways, such as Rap1, prolactin, MAPK, regulation of actin cytoskeleton, and cAMP. These signaling pathways have been reported to be involved in the differentiation of stem cells. Maruyama et al. showed that Rap1 and MAPK signaling are involved in the osteoblast differentiation induced by BMP [57]. Prolactin can act on myeloid progenitors and enhance the differentiation of hematopoietic stem cell differentiation into the NK lineage [68]. Prolactin has a transient effect on the differentiation of the human hippocampal progenitor cell line [69]. Our current results demonstrated that mechanical stress mediates osteogenic/odontogenic differentiation of hDPSCs by regulating the expression of miRNAs. This led to the activation of relevant signaling pathways, and eventually controlled the differentiation of stem cells.

In conclusion, our results identified the differentially expressed miRNA and revealed the target genes and key pathways of osteogenic/odontogenic differentiation of hDPSCs in response to mechanical stress for 7 days. This study may contribute to further investigation of the osteogenic/odontogenic of hDPSCs.

Disclosure of conflict of interest

None.

Address correspondence to: Dr. Jianmin Yang, The Key Laboratory of Shaanxi Province for Craniofacial Precision Medicine Research, College of Stomatology, Xi’an Jiaotong University, Xi’an 710004, Shaanxi, P. R. China. Tel: +86-29-87275706; E-mail:

jianminyang_98@mail.xjtu.edu.cn; Dr. Tiezhou Hou, The Key Laboratory of Shaanxi Province for Craniofacial Precision Medicine Research, College of Stomatology, Xi'an Jiaotong University, Xi'an 710004, Shaanxi, P. R. China; Department of Endodontics, Stomatological Hospital, College of Medicine, Xi'an Jiaotong University, Xi'an 710004, Shaanxi, P. R. China. Tel: +86-29-87280739; E-mail: tiezhou@mail.xjtu.edu.cn

References

[1] Nuti N, Corallo C, Chan B, Ferrari M and Gerami-Naini B. Multipotent differentiation of human dental pulp stem cells: a literature review. Stem Cell Rev Rep 2016; 12: 511-523.

[2] Al-Habib M and Huang GT. Dental mesenchymal stem cells: dental pulp stem cells, periodontal ligament stem cells, apical papilla stem cells, and primary teeth stem cells-isolation, characterization, and expansion for tissue engineering. Methods Mol Biol 2019; 1922: 59-76.

[3] Ge F and Du L. Study and application of multidirectional differentiation potential of dental pulp stem cells. Sheng Wu Yi Xue Gong Cheng Xue Za Zhi 2019; 36: 172-176.

[4] Chen Y, He S, Yan F, Zhou P, Luo K, Zhang Y, Xiao Y and Lin M. Dental pulp stem cells express tendon markers under mechanical loading and are a potential cell source for tissue engineering of tendon-like tissue. Int J Oral Sci 2016; 8: 213-222.

[5] Dong Q, Wang Y, Mohabatpour F, Zheng L, Papagerakis S, Chen D and Papagerakis P. Dental pulp stem cells: isolation, characterization, expansion, and odontoblast differentiation for tissue engineering. Methods Mol Biol 2019; 1922: 91-101.

[6] Han N, Zheng Y, Li R, Li X, Zhou M, Niu Y and Zhang Q. β-catenin enhances odontoblastic differentiation of dental pulp cells through activation of Runx2. PLoS One 2014; 9: e88890.

[7] Sloan AJ and Smith AJ. Stem cells and the dental pulp: potential roles in dentine regeneration and repair. Oral Dis 2007; 13: 151-7.

[8] Cooper PR, Takahashi Y, Graham LW, Simon S, Imazato S and Smith AJ. Inflammation-regeneration interplay in the dentine-pulp complex. J Dent 2010; 38: 687-97.

[9] Millar SE. A pulpy story. Nat Mater 2019; 18: 530-531.

[10] Marrelli M, Codispoti B, Shelton R, Scheven BA, Cooper PR, Tatullo M and Paduano F. Dental pulp stem cell mechanoresponsiveness: effects of mechanical stimuli on dental pulp stem cell behavior. Front Physiol 2018; 9: 1685.

[11] Lee SK, Lee YC, Kook YA, Lee SK and Kim EC. Mechanical stress promotes odontoblastic differentiation via the heme oxygenase-1 pathway in human dental pulp cell line. Life Sci 2010; 86: 107-14.

[12] Accorinte ML, Loguercio AD, Reis A, Carneiro E, Grande RH, Murata SS and Holland R. Response of human dental pulp capped with MTA and calcium hydroxide powder. Oper Dent 2008; 33: 488-95.

[13] Li Z, Cao L, Fan M and Xu Q. Direct pulp capping with calcium hydroxide or mineral trioxide aggregate: a meta-analysis. J Endod 2015; 41: 1412-7.

[14] Schwendicke F, Brouwer F, Schwendicke A and Paris S. Different materials for direct pulp capping: systematic review and meta-analysis and trial sequential analysis. Clin Oral Investig 2016; 20: 1121-32.

[15] Yang L, Yang Y, Wang S, Li Y and Zhao Z. In vitro mechanical loading models for periodontal ligament cells: from two-dimensional to three-dimensional models. Arch Oral Biol 2015; 60: 416-24.

[16] Yu V, Damek-Poprawa M, Nicoll SB and Akintoye SO. Dynamic hydrostatic pressure promotes differentiation of human dental pulp stem cells. Biochem Biophys Res Commun 2009; 386: 661-5.

[17] Mu C, Lv T, Wang Z, Ma S, Ma J, Liu J, Yu J and Mu J. Mechanical stress stimulates the osteo/odontoblastic differentiation of human stem cells from apical papilla via erk 1/2 and JNK MAPK pathways. Biomed Res Int 2014; 2014: 494378.

[18] Hata M, Naruse K, Ozawa S, Kobayashi Y, Nakamura N, Kojima N, Omi M, Katanosaka Y, Nishikawa T, Naruse K, Tanaka Y and Matsubara T. Mechanical stretch increases the proliferation while inhibiting the osteogenic differentiation in dental pulp stem cells. Tissue Eng Part A 2013; 19: 625-33.

[19] Bartel DP. MicroRNAs: genomics, biogenesis, mechanism, and function. Cell 2004; 116: 281-97.

[20] Chen N, Sui B, Hu C, Cao J, Zheng C, Hou R, Yang Z, Zhao P, Chen Q, Yang Q, Jin Y and Jin F. Microrna-21 contributes to orthodontic tooth movement. J Dent Res 2016; 95: 1425-1433.

[21] Zuo B, Zhu J, Li J, Wang C, Zhao X, Cai G, Li Z, Peng J, Wang P, Shen C, Huang Y, Xu J, Zhang X and Chen X. microRNA-103a functions as a mechanosensitive microRNA to inhibit bone formation through targeting Runx2. J Bone Miner Res 2015; 30: 330-45.

[22] Liao J, Zhou X, Zhang Y and Lu H. MiR-1246: a new link of the p53 family with cancer and down syndrome. Cell Cycle 2012; 11: 2624-30.

[23] Chang M, Lin H, Fu H, Wang B, Han G and Fan M. MicroRNA-195-5p regulates osteogenic differentiation of periodontal ligament cells under mechanical loading. J Cell Physiol 2017; 232: 3762-3774.
[24] Li J, Hu C, Han L, Liu L, Jing W, Tang W, Tian W and Long J. MiR-154-5p regulates osteogenic differentiation of adipose-derived mesenchymal stem cells under tensile stress through the Wnt/PCP pathway by targeting Wnt11. Bone 2015; 78: 130-41.
[25] Zhan F, Liu X and Wang X. The role of MicroRNA-143-5p in the differentiation of dental pulp stem cells into odontoblasts by targeting Runx2 via the OPG/RANKL signaling pathway. J Cell Biochem 2018; 119: 536-546.
[26] Xu K, Xiao J, Zheng K, Feng X, Zhang J, Song D, Wang C, Shen X, Zhao X, Wei C, Huang D and Feng G. MiR-21/STAT3 signal is involved in odontoblast differentiation of human dental pulp stem cells mediated by TNF-α. Cell Reprogram 2018; 20: 107-116.
[27] Trejo Iriarte C, Ramírez Ramírez O, Mu?Oz García A, Verdín Terán S and Gómez Clavel J. Isolation of periodontal ligament stem cells from extracted premolars. Simplified method. Rev Odontol (B Aires) 2017; 21: e12-e20.
[28] Tsai A, Hong H, Lin W, Fu J, Chang C, Wang I, Huang W, Weng C, Hsu C and Yen T. Isolation of mesenchymal stem cells from human deciduous teeth pulp. Biomed Res Int 2017; 2017: 2851906.
[29] Ducret M, Farges J, Pasdeloup M, Perrier-Groult E, Mueller A, Mallein-Gerin F and Fabre H. Phenotypic identification of dental pulp mesenchymal stem/stromal cells subpopulations with multiparametric flow cytometry. Methods Mol Biol 2019; 1922: 77-90.
[30] Ashburner M, Ball C, Blake J, Botstein D, Butler H, Cherry J, Davis A, Dolinski K, Dwight S, Eppig J, Harris M, Hill D, Issel-Tarver L, Kasarskis A, Lewis S, Matese J, Richardson J, Ringwald M, Rubin G and Sherlock G. Gene ontology: tool for the unification of biology. The Gene Ontology Consortium. Nat Genet 2000; 25: 25-9.
[31] Mao X, Cai T, Olyarchuk J and Wei L. Automated genome annotation and pathway identification using the KEGG Orthology (KO) as a controlled vocabulary. Bioinformatics 2005; 21: 3787-93.
[32] Young M, Wakefield M, Smyth G and Oshlack A. Gene ontology analysis for RNA-seq: accounting for selection bias. Genome Biol 2010; 11: R14.
[33] Livak K and Schmittgen T. Analysis of relative gene expression data using real-time quantitative PCR and the 2(-Delta Delta C(T)) method. Methods 2001; 25: 402-8.
[34] Lu Y, Zhao Q, Liu Y, Zhang L, Li D, Zhu Z, Gan X and Yu H. Vibration loading promotes osteogenic differentiation of bone marrow-derived mesenchymal stem cells via p38 MAPK signaling pathway. J Biomech 2018; 71: 67-75.
[35] Kraft D, Bindslev D, Melsen B and Klein-Nulend J. Human dental pulp cells exhibit bone cell-like responsiveness to fluid shear stress. Cytotherapy 2011; 13: 214-26.
[36] Han M, Seo Y, Yoon H, Song K and Park J. Effect of mechanical tension on the human dental pulp cells. Biotechnol Bioproc E 2008; 13: 410-417.
[37] Gao Q, Walmsley A, Cooper P and Scheven B. Ultrasound stimulation of different dental stem cell populations: role of mitogen-activated protein kinase signaling. J Endod 2016; 42: 425-31.
[38] Yang H, Shu Y, Wang L, Zou W, Guo L, Shao M, Gao Q and Hu T. Effect of cyclic uniaxial compressive stress on human dental pulp cells in vitro. Connect Tissue Res 2018; 59: 255-262.
[39] Yu J, Xie Y, Xu D and Zhao S. Effect of cyclic strain on cell morphology, viability and proliferation of human dental pulp cells in vitro. Shanghai Kou Qiang Yi Xue 2009; 18: 599-603.
[40] Ji J, Sun W, Wang W, Munyombwe T and Yang X. The effect of mechanical loading on osteogenesis of human dental pulp stromal cells in a novel in vitro model. Cell Tissue Res 2014; 358: 123-33.
[41] Gao Q, Cooper P, Walmsley A and Scheven B. Role of piezo channels in ultrasound-stimulated dental stem cells. J Endod 2017; 43: 1130-1136.
[42] Tan X and Dai Q. Characterization of microRNAs expression profiles in human dental-derived pluripotent stem cells. PLoS One 2017; 12: e0177832.
[43] Feng S, Zhu X, Fan B, Xie D, Li T and Zhang X. miR-19a-3p targets PMEPA1 and induces prostate cancer cell proliferation, migration and invasion. Mol Med Rep 2016; 13: 4030-8.
[44] Wa Q, Li L, Lin H, Peng X, Ren D, Huang Y, He P and Huang S. Downregulation of miR-19a-3p promotes invasion, migration and bone metastasis via activating TGF-β signaling in prostate cancer. Oncol Rep 2018; 39: 81-90.
[45] Zhang S, Li G, Liu C, Lu S, Jing Q, Chen X, Zheng H, Ma H, Zhang D, Ren S, Shen Z, Wang Y, Lu Z, Huang D, Tan P, Chen J, Zhang X, Qiu Y and Liu Y. miR-30e-5p represses angiogenesis and metastasis by directly targeting AEG-1 in squamous cell carcinoma of the head and neck. Cancer Sci 2020; 111: 356-368.
[46] Ma Y, Zhang H, Li X and Liu Y. MiR-30e-5p inhibits proliferation and metastasis of nasopharyngeal carcinoma cells by target-ing USP22. Eur Rev Med Pharmacol Sci 2018; 22: 6342-6349.
[47] Xu G, Cai J, Wang L, Jiang L, Huang J, Hu R and Ding F. MicroRNA-30e-5p suppresses non-small cell lung cancer tumorigenesis by regu-

lating USP22-mediated Sirt1/JAK/STAT3 signaling. Exp Cell Res 2018; 362: 268-278.
[48] Fan X, Luo Y, Wang J and An N. miR-154-3p and miR-487-3p synergistically modulate RHOA signaling in the carcinogenesis of thyroid cancer. Biosci Rep 2020; 40: BSR20193158
[49] Chang C, Liu T, Huang Y, Qin W, Yang H and Chen J. MicroRNA-134-3p is a novel potential inhibitor of human ovarian cancer stem cells by targeting RAB27A. Gene 2017; 605: 99-107.
[50] Parsi S, Soltani B, Hosseini E, Tousi S and Mowla S. Experimental verification of a predicted intronic microRNA in human NGFR gene with a potential pro-apoptotic function. PLoS One 2012; 7: e35561.
[51] Hassanlou M, Soltani B and Mowla S. Expression and function of hsa-miR-6165 in human cell lines and during the NT2 cell neural differentiation process. J Mol Neurosci 2017; 63: 254-266.
[52] Hassanlou M, Soltani B, Medlej A, Kay M and Mowla S. Hsa-miR-6165 downregulates insulin-like growth factor-1 receptor (IGF-1R) expression and enhances apoptosis in SW480 cells. Biol Chem 2020; 401: 477-485.
[53] Francone E, Gentilli S, Santori G, Stabilini C, Fornaro R and Frascio M. MicroRNAs differential expression profile in metastatic colorectal cancer: a pilot study with literature review. Surg Oncol 2021; 37: 101524.
[54] Kim S, Bae W, Ahn J, Heo J, Kim K, Choi K, Sung C and Lee D. MicroRNA signatures associated with lymph node metastasis in intramucosal gastric cancer. Mod Pathol 2021; 34: 672-683.
[55] Zhang Y, Shi X, Zhang J, Chen X, Zhang P, Liu A and Zhu T. A comprehensive analysis of somatic alterations in Chinese ovarian cancer patients. Sci Rep 2021; 11: 387.
[56] Fernandes G, Galbiatti-Dias A, Ferreira L, Serafim Junior V, Rodrigues-Fleming G, De Oliveira-Cucolo J, Biselli-Chicote P, Kawasaki-Oyama R, Maniglia J, Pavarino É and Goloni-Bertollo E. Anti-EGFR treatment effects on laryngeal cancer stem cells. Am J Transl Res 2021; 13: 143-155.
[57] Maruyama T, Jiang M, Abbott A, Yu H, Huang Q, Chrzanowska-Wodnicka M, Chen E and Hsu W. Rap1b is an effector of Axin2 regulating crosstalk of signaling pathways during skeletal development. J Bone Miner Res 2017; 32: 1816-1828.
[58] Li J, Li Y, Wang S, Che H, Wu J and Ren Y. miR-101-3p/Rap1b signal pathway plays a key role in osteoclast differentiation after treatment with bisphosphonates. BMB Rep 2019; 52: 572-576.
[59] Wu M, Wang Y, Shao J, Wang J, Chen W and Li Y. Cbfβ governs osteoblast-adipocyte lineage commitment through enhancing β-catenin signaling and suppressing adipogenesis gene expression. Proc Natl Acad Sci U S A 2017; 114: 10119-10124.
[60] Xia C, Jiang T, Wang Y, Chen X, Hu Y and Gao Y. The p53/miR-145a axis promotes cellular senescence and inhibits osteogenic differentiation by targeting Cbfb in mesenchymal stem cells. Front Endocrinol (Lausanne) 2021; 11: 609186.
[61] Fukuda T, Ochi H, Sunamura S, Haiden A, Bando W, Inose H, Okawa A, Asou Y and Takeda S. MicroRNA-145 regulates osteoblastic differentiation by targeting the transcription factor Cbfb. FEBS Lett 2015; 589: 3302-8.
[62] Chen Y, Zhou F, Liu H, Li J, Che H, Shen J and Luo E. SIRT1, a promising regulator of bone homeostasis. Life Sci 2021; 269: 119041.
[63] Lee H, Suh J, Kim A, Lee Y, Park S and Kim J. Histone deacetylase 1-mediated histone modification regulates osteoblast differentiation. Mol Endocrinol 2006; 20: 2432-43.
[64] Iyer S, Han L, Bartell S, Kim H, Gubrij I, De Cabo R, O'brien C, Manolagas S and Almeida M. Sirtuin1 (Sirt1) promotes cortical bone formation by preventing β-catenin sequestration by FoxO transcription factors in osteoblast progenitors. J Biol Chem 2014; 289: 24069-78.
[65] Hisahara S, Chiba S, Matsumoto H, Tanno M, Yagi H, Shimohama S, Sato M and Horio Y. Histone deacetylase SIRT1 modulates neuronal differentiation by its nuclear translocation. Proc Natl Acad Sci U S A 2008; 105: 15599-604.
[66] Joe I, Jeong S and Cho G. Resveratrol-induced SIRT1 activation promotes neuronal differentiation of human bone marrow mesenchymal stem cells. Neurosci Lett 2015; 584: 97-102.
[67] Songsaad A, Gonmanee T, Ruangsawasdi N, Phruksaniyom C and Thonabulsombat C. Potential of resveratrol in enrichment of neural progenitor-like cell induction of human stem cells from apical papilla. Stem Cell Res Ther 2020; 11: 542.
[68] Tufa D, Shank T, Yingst A, Trahan G, Shim S, Lake J, Woods R, Jones K and Verneris M. Prolactin acts on myeloid progenitors to modulate SMAD7 expression and enhance hematopoietic stem cell differentiation into the NK cell lineage. Sci Rep 2020; 10: 6335.
[69] Smeeth D, Kourouzidou I, Duarte R, Powell T and Thuret S. Prolactin, estradiol and testosterone differentially impact human hippocampal neurogenesis in an in vitro model. Neuroscience 2021; 454: 15-39.

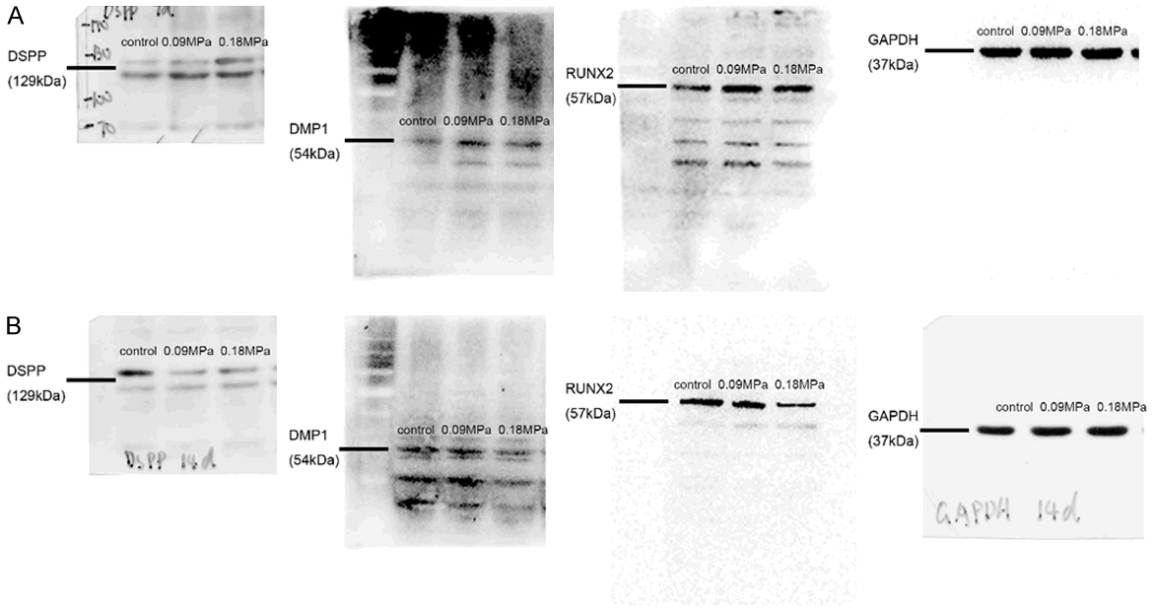

Figure S1. The original western blot images corresponding to the representative images. A. Photographs of the original western blot images showing expression levels of each protein after treatment with 0.09 MPa and 0.18 MPa mechanical stress for 7 days in **Figure 4A**. B. Photographs of the original western blot images showing expression levels of each protein after treatment with 0.09 MPa and 0.18 MPa mechanical stress for 14 days in **Figure 4B**.

Table S1. The primer sequences of predicted target genes (hub genes) for specific quantitative real-time polymerase chain reaction

Genes	Primers	Primer sequence (5'---3')
Hsa-KRAS	Forward	TGTGGTAGTTGGAGCTGGTG
Hsa-KRAS	Reverse	TGACCTGCTGTGTCGAGAAT
Hsa-SIRT1	Forward	GCAGATTAGTAGGCGGCTTG
Hsa-SIRT1	Reverse	TCTGGCATGTCCCACTATCA
Hsa-SOCS3	Forward	GCCACCTACTGAACCCTCCT
Hsa-SOCS3	Reverse	ACGGTCTTCCGACAGAGATG
Hsa-KLHL20	Forward	AACCAACCAGTGGTCTCCAG
Hsa-KLHL20	Reverse	TAGCCGACGGTAATTCATCC
Hsa-RAP1B	Forward	TCCATCACAGCACAGTCCAC
Hsa-RAP1B	Reverse	AATTTGCCGCACTAGGTCAT
Hsa-CBFB	Forward	CCGACCAGAGAAGCAAGTTC
Hsa-CBFB	Reverse	GAATCATGGGAGCCTTCAAA
Hsa-GAPDH	Forward	GCACCGTCAAGGCTGAGAAC
Hsa-GAPDH	Reverse	TGGTGAAGACGCCAGTGGA

Table S2. Actual statistical analysis method for each figure

Figures	Statistical analysis method	Data
Figure 2A	Multiple Student's -test	M±SD
Figure 2Bb, 2Bd	Unpaired Student's t-test	M±SD
Figure 3Ab, 3Ad, 3Bb, 3Bd	Unpaired Student's t-test	M±SD
Figure 4Ab-d, 4Bb-d	Unpaired Student's t-test	M±SD
Figure 5C	Unpaired Student's t-test	M±SD
Figure S2A-C	Unpaired Student's t-test	M±SD

Note: mean ± standard deviation (M±SD).

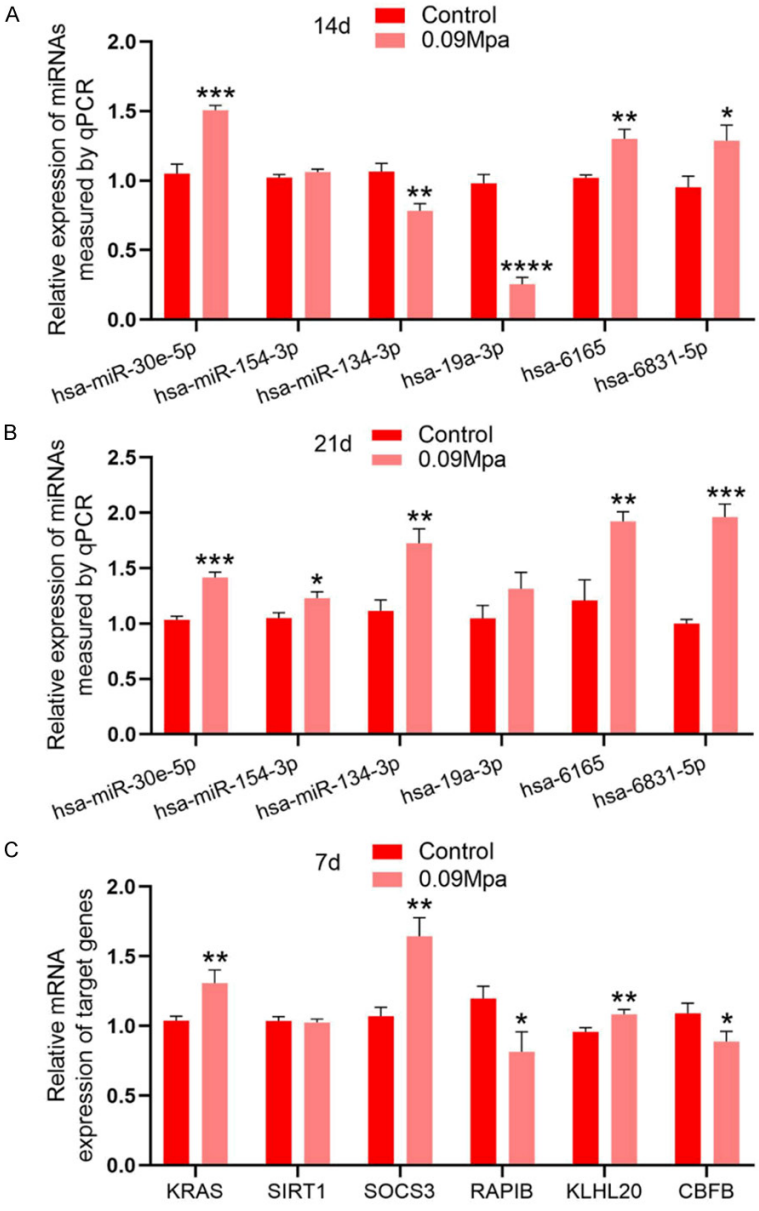

Figure S2. The differentially expressed miRNAs after prolonged exposure and the mRNA expression of predicted target genes. A. Relative expression of differentially expressed miRNAs normalized to U6 in hDPSCs treated with 0.09 MPa mechanical stress for 14 days. B. Relative expression of differentially expressed miRNAs normalized to U6 in hDPSCs treated with 0.09 MPa mechanical stress for 21 days. C. The mRNA expression of six predicated target genes (hub genes) in hDPSCs treated with 0.09 MPa mechanical stress for 7 days. Results were analyzed by unpaired Student's t test. Data are presented as mean ± standard deviation. $^{*}P<0.05$, $^{**}P<0.01$, $^{***}P<0.001$, $^{****}P<0.0001$ when comparing to control.